



Investigating the Effect of Variable Hydrogen Blending on Exergy Destruction in Diesel Engine: An Energy and Exergy Analysis.

Yogesh S. D.

Department of Mechanical Engineering
SRM Institute of Science and
Technology
Chengalpattu, India
yy4505@srmist.edu.in

Phavan Kumar J. S.

Department of Mechanical Engineering
SRM Institute of Science and
Technology
Chengalpattu, India
pj4565@srmist.edu.in

Praveena V.

Department of Mechanical Engineering
SRM Institute of Science and
Technology
Chengalpattu, India
praveenv1@srmist.edu.in

Abstract—This study investigates the impact of hydrogen on engine performance, combustion, and pollutant emissions in a Kirloskar TV1 DI Diesel engine. The engine was operated at a constant rpm of 1500 and output of 5.20 kW, with varying loads ranging from 0.01 kg to 18 kg, using hydrogen at rates ranging from 4 to 10 liter per minute (LPM) as a fuel additive. Energy analysis was performed to pinpoint the origins and magnitude of thermodynamic irreversibility in the engine, followed by an exergy analysis to assess the exergy availability and destroyed availability levels, a comprehensive understanding of the system's performance can be obtained. The study's outcomes indicated that the major contributors to the energy losses, amounting to nearly 40%, were the exhaust gases and cooling water. Meanwhile, the primary source for exergy destruction was heat transfer loss, which was curbed by 25% by introducing hydrogen at a rate of 10 LPM. The investigation also identified that 10 LPM had the highest exergy efficiency, which can serve as a basis for optimizing engine performance and reducing its ecological impact. Moreover, the study demonstrated that introducing hydrogen led to a significant improvement in exergy extraction, recovering almost 50% of the exergy lost through exhaust gases. This approach proved to be a feasible method for exergy recovery. Based on the findings, this study offers valuable insights into how the incorporation of hydrogen can mitigate energy losses and unlock the exergy potential from heat transfer losses.

Keywords—exergy, energy, irreversibility, heat transfer loss

I. INTRODUCTION

As the demand for energy continues to grow and concerns over climate change escalate, researchers are exploring alternative sources of fuel to power vehicles. Although nonrenewable resources like fossil fuels remain the primary source of energy, their limited supply and harmful emissions have led experts to consider alternative options, such as hydrogen [1]. While hydrogen fuel cells have shown promise, their limited cost-effectiveness and logistical challenges have hindered their widespread adoption. Therefore, there is a growing interest in alternative options

like hydrogen-diesel-powered vehicles, which offer several advantages over traditional hydrogen fuel cells. Hydrogen-diesel engines are less costly than fuel cells, primarily due to the latter's expensive materials and intricate manufacturing processes. While the costs of both technologies are reducing, hydrogen fuel cells still require specialized infrastructure, including a broader network of refuelling stations. In contrast, hydrogen-diesel engines can take advantage of the existing diesel refuelling infrastructure with some modifications to the engine and fuel system. As a result, hydrogen-diesel-powered vehicles are more adaptable, cost-effective, and easier to integrate into the current transportation system. Due to its high combustion efficiency and low emissions, hydrogen is an ideal fuel for blending with other fuels. The inclusion of hydrogen in fuel blends has demonstrated the ability to enhance engine efficiency, and keep NO_x emissions at an optimal level [2]. Due to its higher flammability, hydrogen was found to decrease both the ignition delay and combustion duration, ultimately resulting in complete combustion [3].

By conducting an energy analysis, it is possible to identify the inefficiencies occurring in an engine, which provides insight into its overall performance. Additionally, exergy analysis can be carried out to determine the potential of the fuel and the quantity of losses that can be regained, resulting in a more comprehensive understanding of the available exergy [4].

Through experimentation with exergy and energy analysis, Panigrahi et al. found that the use of diesel and mahua biodiesel blends in a diesel engine resulted in a higher level of destroyed exergy compared to pure diesel fuel [5]. Habibian, Karami, and Hoseinpour [6] investigated the impact of soybean biodiesel concentration (20%, 40%, and 100%) in diesel-biodiesel blends on the energy and exergy efficiency of a direct injection (DI) diesel engine, revealing a slight reduction in engine efficiency as combustion irreversibility increased due to the biodiesel proportion increased. Santoso, Bakar, and Nur [7] investigated a dual fuel engine that combines diesel and hydrogen fuels at flow



rates of 21.4, 36.2, and 49.6 LPM at a low load has resulted in significant reductions in diesel consumption, ranging from 50% to 97%. Gözmen Şanlı and Uludamar [8] investigated the impact of diesel, hazelnut biodiesel, and canola biodiesel fuels, and found that the lowest destruction levels were 45.45%, 47.36%, and 47.41% for the diesel, hazelnut biodiesel, and canola biodiesel fuels, respectively. Xia et al. investigated the impact of hydrogen fuel, added at a constant fraction of 25%, to the castor oil biodiesel blends enriched with nano additives in a CI engine on the performance, combustion, and emissions, finding that the addition of hydrogen led to an improvement in combustion performance and superior brake thermal efficiency [9]. Karagöz et al. studied the impact of hydrogen-diesel dual-fuel usage on the performance, emissions, and combustion of diesel engines, observed that the introduction of hydrogen at 25% and 50% of the total fuel energy resulted in a significant reduction in smoke, CO₂, and CO gaseous emissions but a dramatic increase in nitrogen oxides and hydrocarbons [10]. The performance of a compression ignition (CI) engine fuelled with different ternary blends of biodiesel derived from palm, coconut, and jatropha oil with diesel, and found that the exergy destruction of diesel was lower at low loads, while an increase in the percentage of biodiesel in the blends led to a corresponding increase in exergy destruction compared by Manavalla et al. [11]. Gnanamani et al. examined the impact of diesel-cotton seed oil blends with 5%, 10%, and 15% concentrations on engine exergy transfer and total exergy losses, and found that the total exergy losses decreased to 8.4%, 7.81%, 6.63%, and 5.49% for diesel, CB5, CB10, and CB15 blends [12]. Nazzaland AlDoury [13] found that the exergy destruction rate increased by 4.2% and 8.08% for CB8 and CB15 blends of diesel-corn oil compared to conventional diesel, while the exergy efficiency of conventional diesel was higher than that of CB8 and CB15 by 0.86% and 1.67%, respectively. Yamin, Sheet and Hdaib [14] compared the use of petrol-diesel and biodiesel made from waste cooking oil as fuel sources in direct injection CI engines, and observed that biodiesel has a 10% lower heating value on a weight basis than petrol-diesel, while petrol-diesel fuel experiences a 10-15% higher loss of availability to coolant. Cernat et al. found that the addition of hydrogen to a diesel engine led to a significant decrease in CO emissions of nearly 20%, while the higher lower heating value and faster combustion speed of hydrogen contributed to an increase in thermal efficiency [15]. This study [16] assessed the effects of hydrogen influence on irreversibility in a dual fuel diesel engine, and found that an increase in the gas fuel-air ratio from 0.3 to 0.8 resulted in a decrease in irreversibility from 29.8% to 26.6%. Mirica et al. found that at 40% engine partial load, incorporating hydrogen into diesel fuel resulted in better energy efficiency and reduced pollution compared to using standard diesel fuel alone [17]. Norani et al. investigated the impact of incorporating hydrogen into diesel fuel at varying flow rates, and found that at the highest flow rate of 7 liter/minute, the addition of hydrogen resulted in a reduction of unburnt hydrocarbon (HC), carbon dioxide

(CO₂) and carbon monoxide (CO) emissions by 22.2%, 79.9%, and 21.6%, respectively, when compared to using only diesel fuel as a baseline [18]. Bose, Banerjee, and Deb [19] conducted a performance and combustion analysis on a Direct Injection (DI) diesel engine, and found that as the energy share of hydrogen increased when used in combination with diesel, there was a corresponding decrease in Brake Specific Energy Consumption (BSEC), which reduced up to a maximum of 9% compared to the baseline diesel.

II. EXPERIMENTAL ENGINE SETUP

The experiment was carried out on a vertical water-cooled, single-cylinder, four-stroke diesel engine with technical specifications outlined in Table 1. The engine was coupled with an eddy current type dynamometer for loading purposes, while hydrogen injection rates were systematically varied from 4 LPM to 10 LPM. A standalone panel box was utilized and included an air filter housing, fuel tank, manometer, fuel measuring unit, and transmitters for air and fuel sensor, as well as an engine gauge. The cooling water and calorimeter water flow rates were measured using rotameters.

The process of supplying hydrogen to an engine involves storing it in a high-pressure tank and regulating its pressure through a flow control valve with a flame arrestor, which ensures that there is no backfire into the hydrogen storage tank. Hydrogen is then injected into the engine via the intake engine specifications manifold, with the aid of a flow meter that measures and controls the injection rate to form a uniform mixture. Fuel properties of hydrogen and diesel are given in Table 2.

TABLE I. ENGINE SPECIFICATIONS

Attributes	Specifications
Model	Kirloskar TV1 engine
Maximum power (kW)	5.2
Rated speed (r.p.m)	1500
Bore (mm) × stroke (mm)	87.5 × 110
Compression ratio	17.5:1
Hydrogen injection system	Manifold injection
Connecting rod length (mm)	234
Swept volume (cm ³)	661.45

TABLE II. FUEL PROPERTIES OF HYDROGEN AND DIESEL

Fuel Properties	Hydrogen	Diesel
Density (kg/m ³)	89.88	820
Lower heating value (MJ/kg)	120	42.31
Autoignition temperature (°C)	585	210
Carbon content (%)	0	84
Calorific value (MJ/kg)	142	45.5
Ignition energy (mJ)	0.011	20

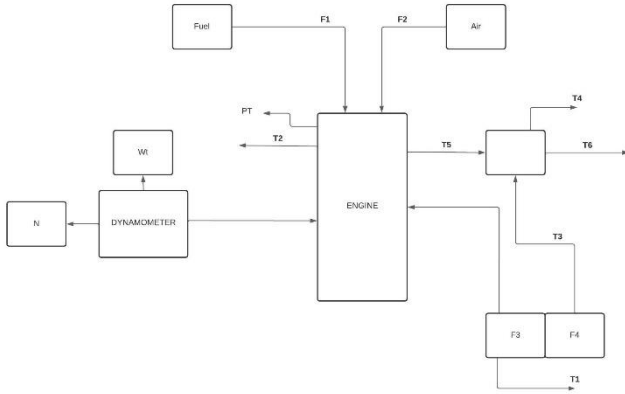


Fig. 1. Experimental engine setup

The experimental setup schematic diagram is presented in Fig. 1, depicting F1 as the fuel injector, F2 as the air flow sensor, PT as the pressure transducer, N as the crankshaft position sensor (CPS), which plays a crucial role in the ignition system of an engine by providing the engine control module (ECM) with vital data on the speed and position of the crankshaft, and F3 and F4 as the rotameters. The engine cooling water inlet and outlet are represented by T1 and T2, respectively, while T3 and T4 denote the calorimeter water inlet and outlet. Lastly, T5 and T6 correspond to the exhaust gas inlet and outlet, respectively.

III. METHODOLOGY

A. Energy Analysis

The energy balance or heat balancesheet is a method utilized to analyse and quantify the energy flow within a given system or process. The data is presented in a tabular format, which details the energy inputs, outputs, and losses along with their respective quantities and units of measurement.

The main objective of creating an energybalancesheet is to verify that the total energy entering the system is equivalent to the total energy leaving the system, in line with the firstlaw of thermodynamics. This technique can assist in identifying areas where energy losses occur and improving the overall efficiency of the process or system.

$$Q_s = Q_{bp} + Q_{cw} + Q_{ex} + Q_u, \quad (1)$$

1) *Energy input*: The amount of energy that is supplied to the engine (Q_s) in kW, is

$$Q_s = m_f \times L.C.V., \quad (2)$$

where, m_f represents the mass of fuel that is provided to the engine in kg/hr, $L.C.V.$ denotes the fuel's lower calorific value in kJ/kg.

2) *Brake power*: The amount of energy that is converted into useful work, referred to as the output power (Q_{bp}) in kW, is

$$Q_{bp} = \frac{2 \times \pi \times N \times T}{60 \times 1000}, \quad (3)$$

where, N represents the rate of crankshaft revolutions per minute, T denotes the torque that is generated by the system in N·m.

3) *Cooling water loss*: The amount of energy that is dissipated through the cooling water (Q_{cw}) in kW, is

$$Q_{cw} = m_{we} \times C_{pw} \times (T_2 - T_1), \quad (4)$$

where, m_{we} represents the mass of cooling water that circulates through the engine's cooling jacket in kg/hr, C_{pw} denotes the specific heat of water, which has a value of 4.187 kJ/kg·K, $(T_2 - T_1)$ refers to the temperature difference of the water as it passes through the engine's cooling jacket in K.

4) *Exhaust gases loss*: The amount of energy that is dissipated through the exhaust gases (Q_{ex}) in kW, is

$$Q_{ex} = m_{ge} \times C_{pe} \times (T_5 - T_a), \quad (5)$$

where, m_{ge} represents the mass of exhaust gases in kg/hr, C_{pe} denotes the specific heat of exhaust gas, which has a value of 1.063 kJ/kg·K, T_5 refers to the temperature of the exhaust gases as it enters the calorimeter in K, T_a represents the ambient temperature in K.

5) *Unaccounted energy losses*: The energy quantity that exits a system but is not considered during energy balance computations, as it occurs due to factors such as radiation and convection.

The amount of energy that is lost through unidentified mechanisms (Q_u) in kW, is

$$Q_u = Q_s - (Q_{bp} + Q_{cw} + Q_{ex}), \quad (6)$$

B. Exergy Analysis

An exergy analysis is conducted after an energy analysis to determine the amount of exergy that can be regained from heat losses and the amount of exergy destruction that is irreversible, resulting in permanent losses.

$$e_f^{ch} = e_{heat} + e_w + e_o + e_d, \quad (7)$$

1) *Exergy input*: The amount of exergy that is supplied to the engine (e_f^{ch}) in kW, is



$$e_f^{ch} = m_d \times e_d^{ch} + m_h \times e_h^{ch}, \quad (8)$$

where, m_d stands for the mass of diesel fuel that has been supplied in kg/hr, e_d^{ch} represents the specific chemical exergy of the diesel fuel in kJ/kg, m_h stands for the mass of hydrogen injected in kg/hr, e_h^{ch} represents the specific chemical exergy of hydrogen in kJ/kg.

Given that the relative humidity of the air is zero and its temperature is identical to the reference temperature of 300 K, the air contribution to the exergy input is negligible.

2) *Heat losses*: It refers to the measurement of exergy that is lost as waste heat, rather than being converted into useful work within a system.

Exergy transfer associated with heat loss (e_{heat}) in kW, is

$$e_{heat} = \sum \left(1 - \frac{T_0}{T_{cw}} \right) \times Q_{loss}, \quad (9)$$

where, T_{cw} refers to the average temperature of the outlet and inlet cooling in K, T_0 is temperature of the dead state in K, Q_{loss} is the rate of heat transfer out of each component in the engine in kW.

$$Q_{loss} = e_f^{ch} - (W + e_{eg}^{ch}), \quad (10)$$

where, W refers to the output power in kW, e_{eg}^{ch} represents the specific chemical exergy of the exhaust gases in kW.

$$e_{eg}^{ch} = \bar{R} \times T_0 \sum_{i=1}^n a_i \ln \left(\frac{Y_i}{Y_i^e} \right), \quad (11)$$

where \bar{R} stands for the universal gas constant, which has a value of 0.287 kJ/kmol-K, Y_i represents the molar ratio of the i th component in the exhaust gases, Y_i^e represents the molar ratio of the i th component in the reference environment.

The molar fractions of N₂, O₂, Ar, CO₂, Ne, He, and H₂O in the reference environment are 0.7561%, 0.2028%, 0.0091%, 0.0003%, 1.77×10⁻⁵%, 5.08×10⁻⁶%, and 0.03167%, respectively, indicating the composition of the atmosphere [20].

3) *Work rate*: Exergy transfer associated with work rate (e_w) in kW, is

$$e_w = W - P_0(V_2 - V_1), \quad (12)$$

where, P_0 is atmospheric pressure in bar, ($V_2 - V_1$) is change in volume.

When there is a change in volume within a system, the exergy accompanying the work done by the system would

not be the same as the output power of the system. However, in the case of an engine, it can be considered a closed system, where the exergy accompanying the work would be equal to the work done by the system.

4) *Exergy output*: Exergy output refers to the complete exergy that can be recuperated, encompassing the exergy that can be obtained from exhaust gases and cooling water. Effectively, it denotes the entire potential exergy that can be derived from a system, considering all feasible sources.

Exergy output (e_o) in kW, is

$$e_o = m_f \times (e_{im} + e_{eg}^{ch}), \quad (13)$$

where, e_{im} refers to the exhaust specific thermo-mechanical exergy in kW.

$$e_{im} = (h - h_0) - T_0(S - S_0), \quad (14)$$

where, h refers to the enthalpy of the system in kJ/kg, h_0 refers to the enthalpy of the system at a reference state in kJ/kg, S refers to the entropy of the system in kJ/kg·K, S_0 refers to the entropy of the system at a reference state in kJ/kg·K.

5) *Exergy destruction*: Exergy transfer linked to irreversibility (e_d) in kW, is

$$e_d = e_f^{ch} - e_w - e_{heat} - e_o, \quad (15)$$

C. Exergy Availability

The exergy available from the identified sources of loss, such as cooling water and exhaust gases, encompasses the exergy that can be availed from the shaft too.

$$e_f^{ch} = A_s + (A_{cw} + A_{ex}) + A_d, \quad (16)$$

1) *Shaft availability*: The quantity of exergy that can be obtained through a shaft (A_s) in kW, is

$$A_s = e_w, \quad (17)$$

2) *Cooling water exergy availability*: The quantity of exergy that can be obtained through the cooling water (A_{cw}) in kW, is

$$A_{cw} = Q_{cw} - [m_{we} \times C_{pw} \times T_a \times \ln \left(\frac{T_2}{T_1} \right)], \quad (18)$$

3) *Exhaust gases exergy availability*: The exergy present in the exhaust gases represents the exergy that could have been recovered but is lost during the exhaust process. This means that it is the exergy that has the potential to be



extracted from the exhaust gases and utilized, instead of being wasted as a result of heat loss.

Exhaust gases exergyavailability (A_{ex}) in kW, is

$$A_{ex} = Q_{ex} - \left[m_{ge} \times T_a \times \left\{ C_{pe} \ln \left(\frac{T_5}{T_a} \right) - \bar{R} \times \ln \left(\frac{P_e}{P_a} \right) \right\} \right] + e_{eg}^{ch}, \quad (19)$$

where, P_a denotes the ambient pressure in bar, P_e denotes the final pressure of exhaust gases in bar.

4) *Destructed availability*: Destructed availability refers to the exergy that cannot be recovered due to either unknown sources of loss or inevitable heat losses that occur in engine, such as those from the exhaust gases and cooling water.

Destructed Availability (A_d) in kW, is

$$A_d = e_f^{ch} - (A_s + A_{cw} + A_{ex}), \quad (20)$$

D. Exergy Efficiency

1) *Efficiency assessed via work rate*: Exergy efficiency refers to the ratio between the useful work produced and the exergy input required to produce it.

Exergy efficiency associated with work rate ($e_w^{\%}$) in %, is

$$e_w^{\%} = \left(\frac{e_w}{e_f^{ch}} \right) \times 100, \quad (21)$$

2) *Efficiency assessed via exergy availability*: The exergy efficiency related to exergy availability pertains to the recoverable exergy from known sources, such as exhaust gases loss and cooling water loss, in relation to the exergy input.

Exergy efficiency associated with exergy availability ($e_a^{\%}$) in kW, is

$$e_a^{\%} = \left(\frac{e_r}{e_f^{ch}} \right) \times 100, \quad (22)$$

where, e_r is exergy recoverable in kW.

IV. RESULTS AND DISCUSSIONS

A. Brake Power, Diesel Consumption, Energy Input and Exergy Input

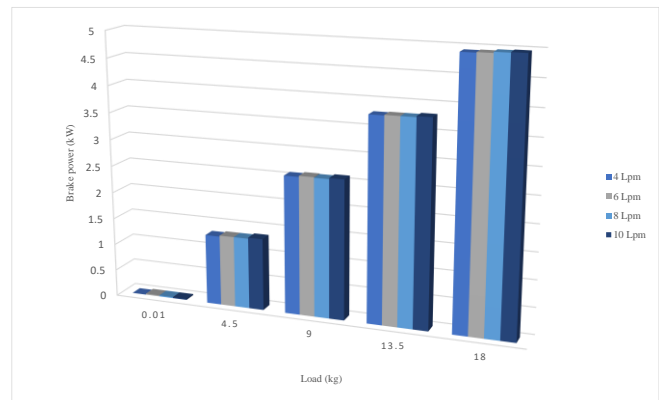


Fig. 2. Brake power versus load

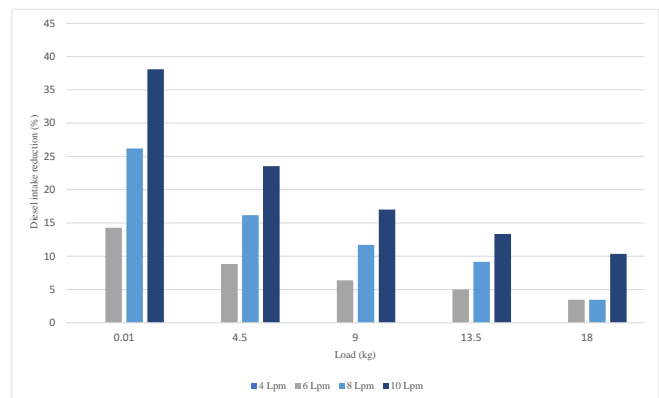


Fig. 3. Diesel intake reduction versus load

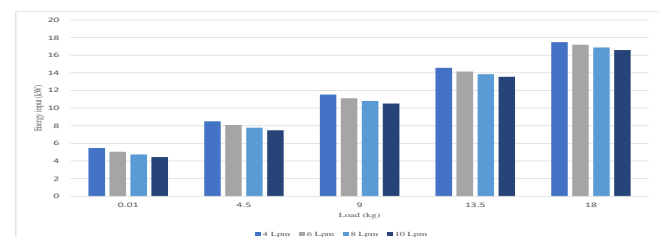


Fig. 4. Energy input versus load

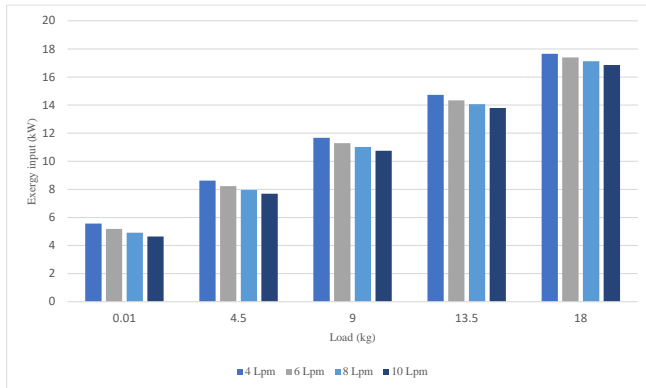


Fig. 5. Exergy input versus load

Fig. 2 demonstrates the variation of brake power with engine loads for variable hydrogen blends. Taking the 18kg load as an example, and at a flow rate of 10 LPM, the diesel consumption rate was observed to decrease by approximately 10.33% compared to a flow rate of 4 LPM. Despite the reduced diesel consumption, the output of brake power remained constant at 4.97 KW.

Fig. 3 demonstrates the variation of diesel intake reduction as a percentage with engine loads for variable hydrogen blends. Under 0.01kg load, the introduction of hydrogen at a flow rate of 10 LPM caused a 38.09% reduction in diesel flow rate compared to a flow rate of 4 LPM. As the load increased to 4.5, 9, 13.5, and 18kg, the diesel flow rate was reduced by 23.52%, 17.02%, 13.33%, and 10.34%, respectively, when compared to the corresponding load at a flow rate of 4 LPM

As a result of the reduction in diesel and air intake due to the introduction of hydrogen, there is a corresponding decrease in both the energy input and exergy input, which is shown in Fig. 4 and Fig. 5. Despite this reduction in input, the brake power output remains consistent, demonstrating the effectiveness of hydrogen incorporation in maintaining optimal power output and compensating for the lost energy and efficiency caused by reduced diesel and air intake.

B. Cooling Water Loss, Exhaust Gases Loss and Unaccounted Energy losses

Fig. 6 demonstrates the variation of cooling water loss with engine loads for variable hydrogen flow rates. A downward trendline was observed, indicating that an increase in hydrogen flow rates results in a corresponding reduction in

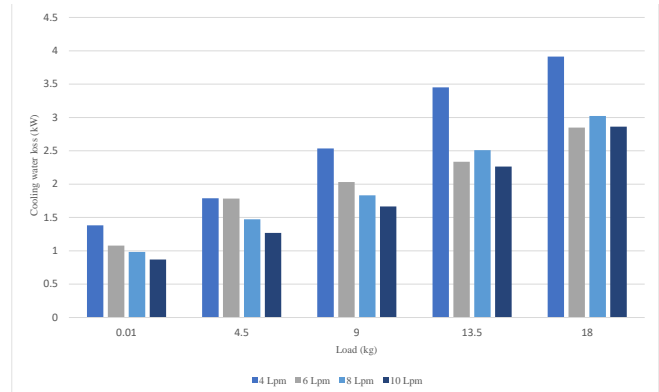


Fig. 6. Cooling water loss versus load

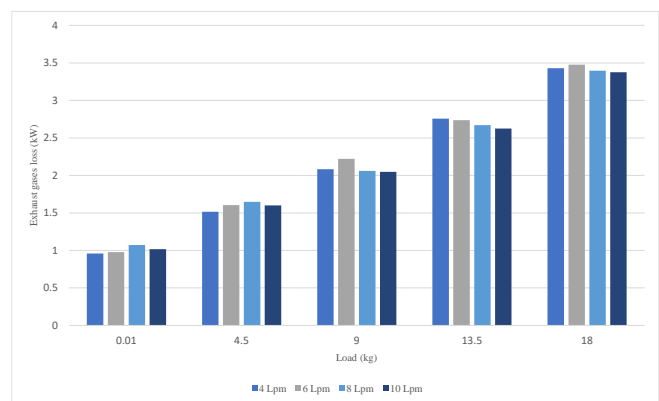


Fig. 7. Exhaust gases loss versus load

cooling water loss. Notably, at a flow rate of 10 LPM, the maximum reduction in cooling water loss was observed.

Fig. 7 displays the relationship between exhaust gases loss and engine loads for hydrogen blends. It was observed that there were gradual fluctuations in exhaust gases loss. Notably, a gradual decrease in exhaust gases loss was observed at a hydrogen injection flow rate of 10 LPM for all loads.

Fig. 8 represents the variation of energy loss with hydrogen flow rates in terms of cooling water loss (Cwl) and energy input. The energy input percentage was scaled down to 50 percent to obtain a clearer view of the results.

To isolate the impact of hydrogen on cooling water loss and examine it solely in terms of energy input, a graphical representation was made. It was observed that as the load and

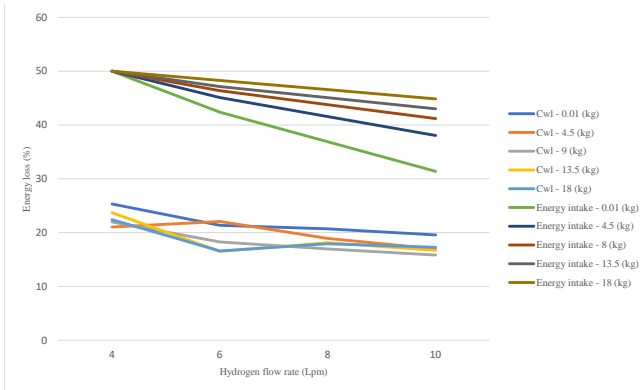


Fig. 8. Energy loss versus hydrogen flow rates in terms of cooling water loss

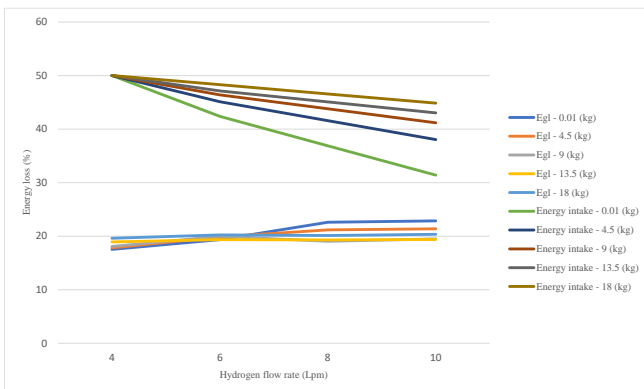


Fig. 9. Energy loss versus hydrogen flow rate in terms of exhaust gases loss

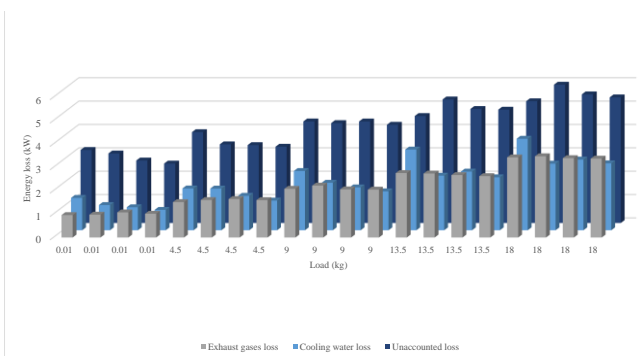


Fig. 10. Energy loss versus load across all sources

hydrogen incorporation increases, the trendline shifts from a curve towards a straight line, indicating that the percentage of energy input reduction decreases compared to the corresponding load at a hydrogen injection rate of 4 LPM.

However, despite this decrease in energy input reduction, the cooling water loss continues to follow a downward trendline instead of rising. This implies that an increase in hydrogen injection flow rate can reduce cooling water loss, even when the energy input increases.

The methodology used in the previous figure has been applied to this Fig. 9 as well, which represents the variation of energy loss with hydrogen flow rates in terms of exhaust gases loss (Egl) and energy input. As load and hydrogen incorporation increases, the trendline of exhaust gases loss shows a downward trend, indicating a reduction in energy loss. At 18 kg load, the energy input trendline approaches a straight-line formation, while the trendline for exhaust gases loss continues to show a downward trend. At a load of 0.01 kg, exhaust gases loss increases noticeably up to 8 LPM, but at a flow rate of 10 LPM, the trendline changes direction and begins to decrease. This suggests that increasing the hydrogen flow rate can reduce exhaust gases loss. Fig. 10 displays the losses attributed to exhaust gases loss, cooling water loss, and unaccounted losses.

C. Availabilities and Exergy Recoverable

Fig. 11 illustrates the relationship between cooling water loss and its exergy availability with respect to hydrogen flow rates. It was observed that at a flow rate of 10 LPM, the cooling water loss reduction is more significant. Additionally, the graph demonstrates that the extraction of exergy from the cooling water loss maintains at an optimal level, indicating an

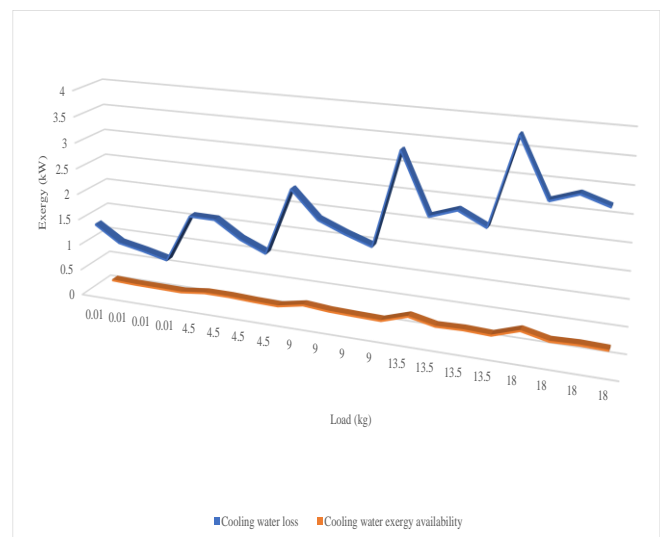


Fig. 11. Exergy versus load in terms of cooling water loss and cooling water exergy availability

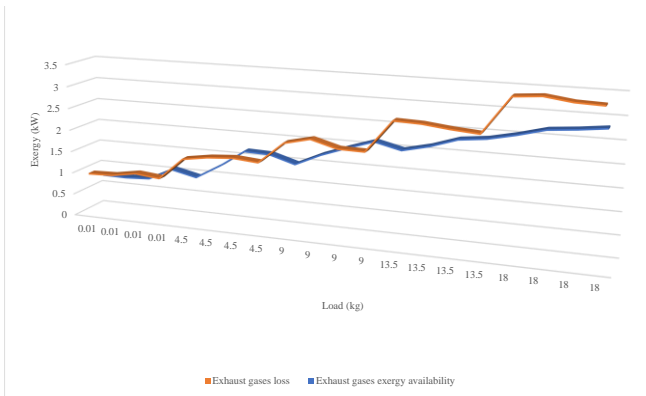


Fig. 12. Exergy versus load in terms of exhaust gases loss and exhaust gases exergy availability

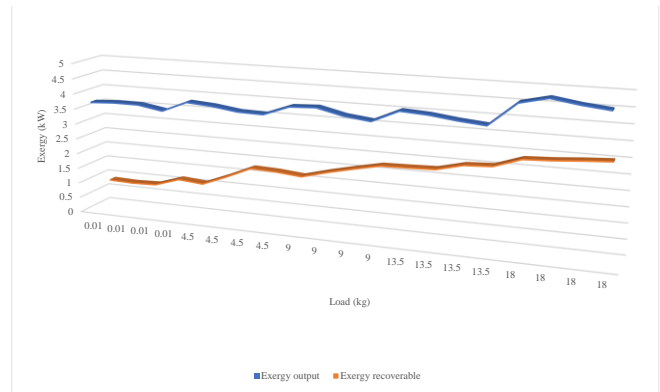


Fig. 14. Exergy versus load in terms of exergy output and exergy recoverable

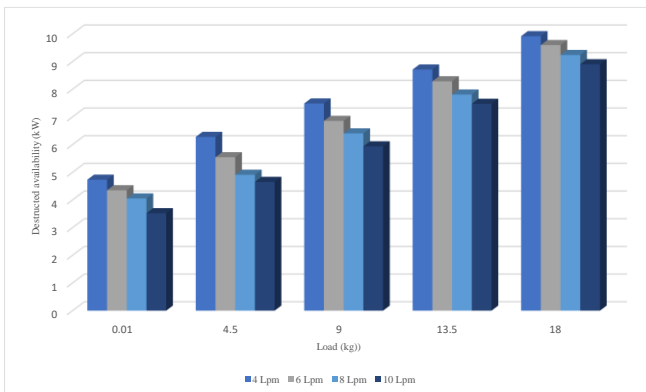


Fig. 13. Destroyed availability versus load

increase in hydrogen incorporation leads to minimal exergy extraction from cooling water loss.

Fig. 12 demonstrates the changes in exhaust gases loss and its corresponding availability in terms of exergy extraction. It was observed that the trend of exhaust gases availability is upward, following the downward trend of exhaust gases loss. The graph depicts that with the increase in hydrogen flow rate, more exergy extraction can be achieved from exhaust gases compared to cooling water. The highest exergy extraction was noted at 10 LPM hydrogen flow rate, which varied between 30% to 60% with an increase in load.

Fig. 13 demonstrates the variation of destroyed availability with engine loads for variable hydrogen blending.

The destroyed availability is significantly lower at 10 LPM of all loads, indicating a higher potential for exergy recovery from the cooling water and exhaust gases.

As LPM increases, exergy recoverable is increasing and exergy output is reducing which means more exergy can be recovered from the exhaust gases loss and cooling water loss, additionally hydrogen adds contribution to reduction in unaccounted loss, as shown in Fig. 14 which depicts the variation of exergy with engine loads in terms of exergy output and exergy recoverable for variable hydrogen blends.

D. Efficiencies

Fig. 15 demonstrates the variation of efficiency assessed via work rate with engine loads for variable hydrogen blends. It was observed that exergy efficiency increases with an increase in hydrogen flow rate. The maximum exergy

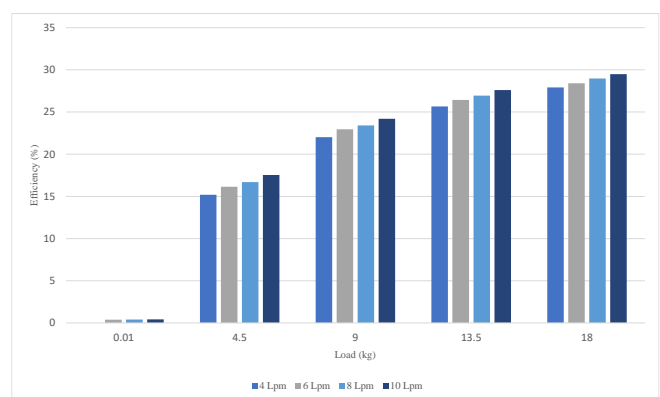


Fig. 15. Work rate efficiency versus load

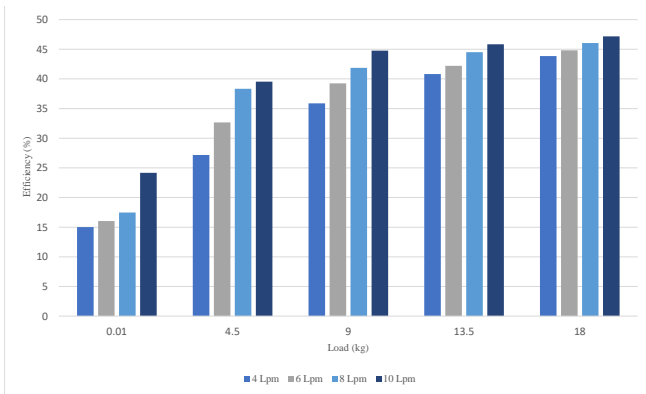


Fig. 16. Exergy availability efficiency versus load

efficiency was observed at 10 LPM hydrogen injection rate. To enhance comprehension, Fig. 16 was generated to depict the exergy availability at various loads as a function of hydrogen flow rate.

E. Emissions

1) *Carbon dioxide emission:* Fig. 17 shows the variation of carbon dioxide emission with engine loads for variable hydrogen blends. It was observed that there is an inverse relationship between hydrogen flow rate and carbon dioxide emission, where an increase in the former leads to a decrease in the latter. This is because the consumption of diesel fuel decreases with an increase in hydrogen flow rate, resulting in lower carbon content. The maximum percentage reduction in carbon dioxide emissions for a given load was observed at a hydrogen flow rate of 10 LPM.

2) *Nitrogen oxides emission:* Fig. 18 shows the variation

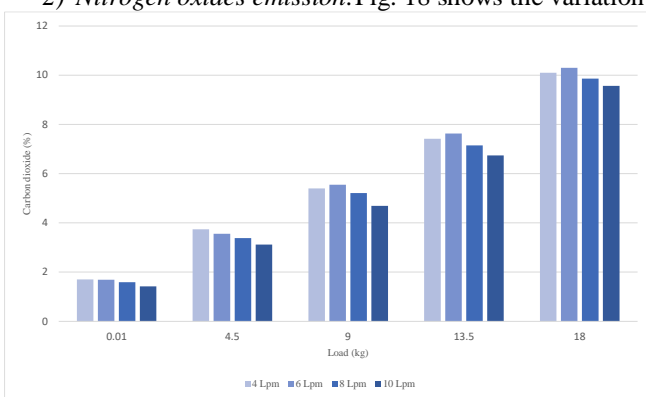


Fig. 17. Carbon dioxide emission versus load

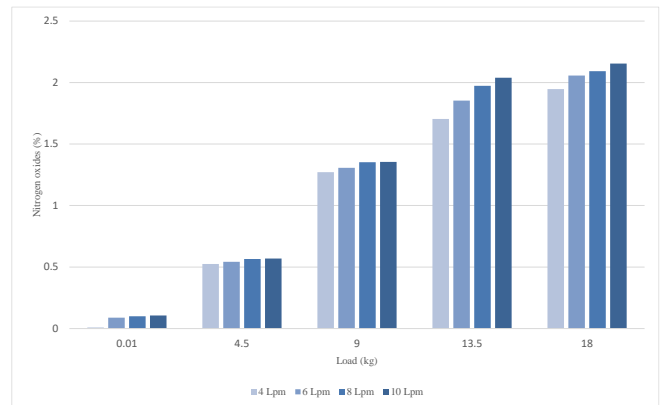


Fig. 18. Nitrogen oxides emission versus load

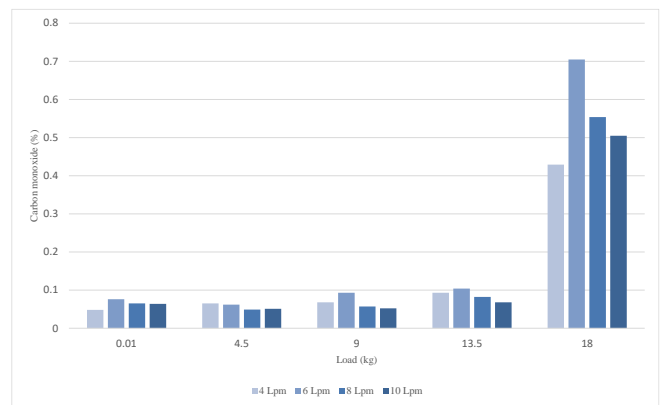


Fig. 19. Carbon monoxide emission versus load

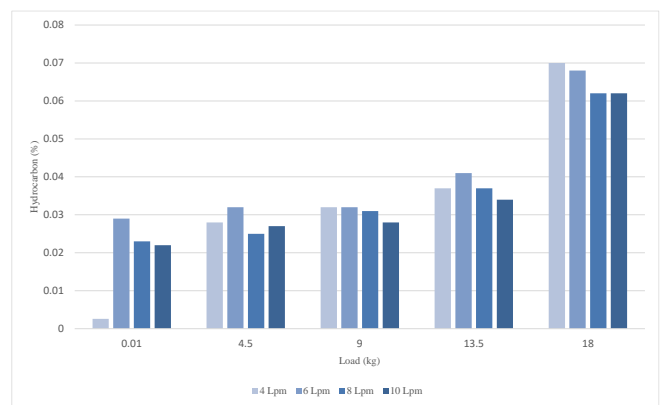


Fig. 20. Hydrocarbon emission versus load



of nitrogen oxides emission with engine loads for variable hydrogen blends, it was observed that there is a positive correlation between the incorporation rate of hydrogen and the emission of nitrogen oxide, as higher hydrogen levels lead to better combustion, resulting in increased temperature and pressure, and subsequently, slightly higher levels of nitrogen oxide emissions.

However, when comparing loads of 18 kg and 13.5 kg, it was observed that the percentage reduction in nitrogen oxide emissions is greater at a hydrogen flow rate of 10 LPM than at 4 LPM, for both loads.

3) *Carbon monoxide emission:* Fig. 19 shows the variation of carbon monoxide emission with engine loads for variable hydrogen blends, there is a reduction in carbon monoxide emissions as the load and hydrogen incorporation increase, due to the improved combustion. The optimal level of carbon monoxide emissions of around 0.1% was maintained from 0.01 kg to 13.5 kg load, and for all loads, the maximum percentage reduction in emissions was observed at a hydrogen flow rate of 10 LPM.

4) *Hydrocarbon emission:* Fig. 20 shows the variation of hydrocarbon emission with engine loads for variable hydrogen blends, it was observed that the emission of hydrocarbons was maintained at an optimal level of approximately 0.03% for loads ranging from 0.01 kg to 13.5 kg. Moreover, an increase in hydrogen flow rate resulted in a reduction in hydrocarbon emissions, indicating its beneficial impact on the emissions reduction.

V. CONCLUSION

An investigation was conducted on a CI engine using diesel hydrogen blends with flow rates ranging from 4 to 10 LPM, and the results indicated that an increase in hydrogen incorporation leads to a decrease in diesel fuel consumption, with reductions of up to 38% observed at 10 LPM compared to 4 LPM at the corresponding loads ranging from 0.01 to 18 kg. The study also revealed a maximum reduction in energy and exergy input at 10 LPM with the same brake power, indicating a decrease in engine losses. Cooling water losses were significantly reduced at 10 LPM, and exhaust gases loss followed a downtrend line relative to the 4 LPM hydrogen flow rate at their corresponding loads. The exergy efficiency associated with work rate exhibited an increasing trendline of around 5% from 4 to 10 LPM, achieving maximum exergy efficiency at 10 LPM. Additionally, increasing the hydrogen flow rate led to an increase in exergy recoverable, meaning more exergy could be extracted through cooling water loss and exhaust gases loss, while exergy output decreased with an increase in hydrogen flow rate, indicating a decrease in exergy recoverable from unknown sources, which was also considered equivalent to exergy destruction. Carbon dioxide emissions decreased, while hydrocarbon and carbon

monoxide remained at an optimal level of emission, with the maximum reduction observed at 10 LPM. However, nitrogen oxide emissions slightly increased due to better combustion, but with an increase in load, the trendline for NO_x emissions changed, revealing a lower percentage increase. The findings demonstrate the crucial role played by hydrogen in reducing diesel fuel consumption while achieving the same work rate and its impact on reducing heat losses and destruction while enhancing exergy extraction.

ACKNOWLEDGMENT

We extend our sincere gratitude to the SVEAC laboratory located in Kanchipuram, India, for their invaluable assistance in facilitating the collection of data for this project. Their expertise and support have been instrumental in the successful completion of our research.

REFERENCES

- [1] H. L. Yipet *et al.*, "A Review of Hydrogen Direct Injection for Internal Combustion Engines: Towards Carbon-Free Combustion," *Applied Sciences*, vol. 9, no. 22, article no. 4842, Nov. 2019.
- [2] J. Ahn, K. Lee, and K. Min, "Effect of Hydrogen Addition on Diesel Engine Performance and Emissions," *International Journal of Engineering Studies*, vol. 9, no. 1, pp. 79-87, 2017.
- [3] N. M. Al-Najem and J. M. Diab, "Energy-Exergy Analysis of a Diesel Engine," *Heat Recovery Systems and CHP*, vol. 12, no. 6, pp. 525-529, Nov. 1992.
- [4] A. Martínez-Rodríguez and A. Abánades, "Comparative Analysis of Energy and Exergy Performance of Hydrogen Production Methods," *Entropy*, vol. 22, no. 11, article no. 1286, Nov. 2020.
- [5] N. Panigrahi, M. K. Mohanty, S. R. Mishra, and R. C. Mohanty, "Performance, Emission, Energy, and Exergy Analysis of a C.I. Engine Using Mahua Biodiesel Blends with Diesel," *International Scholarly Research Notices*, vol. 2014, Oct. 2014.
- [6] S. Habibian, R. Karami, and M. Hoseinpour, "Energy and exergy analyses of combustion process in a DI diesel engine fuelled with diesel-biodiesel blends," *Annals of Mathematics and Physics*, vol. 12, pp. 1-8, Mar. 2021.
- [7] W. B. Santoso, R. A. Bakar, and A. Nur, "Combustion Characteristics of Diesel-Hydrogen Dual Fuel Engine at Low Load," *Energy Procedia*, vol. 32, pp. 3-10, 2013.
- [8] B. Gözmen Şanlı and E. Uludamar, "Energy and exergy analysis of a diesel engine fuelled with diesel and biodiesel fuels at various engine speeds," *Energy Sources, Part A: Recovery, Utilization, and Environmental Effects*, vol. 42, no. 11, pp. 1299-1313, Jun. 2019.
- [9] C. Xia, K. Brindhadevi, A. Elfasakhany, M. Alsehli, and S. Tola, "Performance, combustion and emission analysis of castor oil biodiesel blends enriched with nanoadditives and hydrogen fuel using CI engine," *Fuel*, vol. 306, article no. 121541, Dec. 2021.
- [10] Y. Karagöz, T. Sandalcı, L. Yu'ksek, A. S. Dalkılıç, and S. Wongwises, "Effect of hydrogen-diesel dual-fuel usage on performance, emissions and diesel combustion in diesel engines," *Advances in Mechanical Engineering*, vol. 8, no. 8, article no. 168781401666445, Aug. 2016.
- [11] S. Manavallaet *et al.*, "Exergy Analysis of a CI Engine Operating on Ternary Biodiesel Blends," *Sustainability*, vol. 14, no. 19, article no. 12350, September 2022.



- [12] S. Gnanamani, P. Gaikwad, L. Subramaniam, and R. Chandralingam, "Exergy analysis in diesel engine with binary blends," *Thermal Science*, vol. 26, no. 1 Part A, pp. 353-362, 2022.
- [13] I. T. Nazzal and R. R. J. AlDoury, "Exergy and Energy Analysis of Diesel Engine Fuelled with Diesel and Diesel - Corn Oil Blends," *Journal of Advanced Research in Fluid Mechanics and Thermal Sciences*, vol. 63, no. 1, pp. 92-106, 2019.
- [14] J. A. Yamin, E. A. E. Sheet, and I. Hdaib, "Exergy analysis of biodiesel fueled direct injection CI engines," *Energy Sources, Part A: Recovery, Utilization, and Environmental Effects*, vol. 40, no. 11, pp. 1351-1358, May 2018.
- [15] A. Cernat, C. Pana, N. Negurescu, C. Nutu, D. Fuiurescu, and G. Lazaroiu, "Aspects of an experimental study of hydrogen use at automotive diesel engine," *Heliyon*, vol. 9, no. 3, March 2023.
- [16] S. Jafarmadar, "Exergy analysis of hydrogen/diesel combustion in a dual fuel engine using three-dimensional model," *International Journal of Hydrogen Energy*, vol. 39, no. 17, pp. 9505-9514, June 2014.
- [17] I. Mirica, A. Cernat, C. Pana, N. Negurescu, and C. Nutu, "Performance comparison between hydrogen and diesel fuel fueled compression ignition engine," *U.P.B. Sci. Bull., Series D*, vol. 77, iss. 4, pp. 21-32, 2015.
- [18] M. N. M. Norani, B. T. Tee, Z. M. Zulfattah, M. N. Mansor, and M. I. Ali, "Effect of Continuous Hydrogen Injection on Diesel Engine Performance and Emission," *Int. Rev. Mech. Eng.*, vol. 11, no. 4, pp. 213-218, Apr. 2017.
- [19] P. K. Bose, R. Banerjee, and M. Deb, "Hydrogen combustion in a single cylinder diesel engine and to study its performance and combustion parameters," *Int. J. Mech. & Rob. Res.*, vol. 1, no. 4, pp. 300-308, Oct. 2012.
- [20] Z. Wu, S. Zhou, and L. An, "The Second Law (Exergy) Analysis of Hydrogen," *Journal of Sustainable Development*, vol. 4, no. 1, January 2019.